Dielectronic-recombination rate coefficients for the lithium isoelectronic sequence

D. J. McLaughlin and Yukap Hahn
Department of Physics, University of Connecticut, Storrs, Connecticut 06268
(Received 5 July 1983)

The dielectronic recombination (DR) rate coefficients are calculated in the nonoverlapping resonance approximation for the target ions O^{5+}, Ar^{15+}, Fe^{23+}, and Mo^{39+} at several electron temperatures for the initial state $1s^22s$. The autoionizing and radiative transition probabilities are computed with single-configuration, nonrelativistic Hartree-Fock wave functions and LS coupling. All possible Rydberg autoionizing states and their cascades are included. The relative contributions to the total DR rate of the $1s$, $2s(\Delta n\neq 0)$, and $2s(\Delta n=0;2s\rightarrow 2p)$ transitions are examined for each ion. We find that the main contribution to the DR rate is from $2s$-electron excitation (both $\Delta n\neq 0$ and $\Delta n=0$ processes), although the contribution from $1s$ excitation is found to be as large as 40% of the total rate at high temperatures. Finally, the effect of configuration mixing is examined for a group of dominant states and the effect on the overall rate is estimated.

I. INTRODUCTION

It is now well established that accurate values of dielectronic-recombination (DR) rate coefficients, together with the ionization rates, are necessary for precise determination of the characteristics of high-temperature low-density plasmas of solar corona and present-day tokamaks. In tokamak plasma machines metal atoms from the primary container walls and the current limiter are sputtered into the plasma where they are stripped to high degrees of ionization.[1] Noble-gas atoms are also introduced into the plasma for diagnostic purposes. The recombining ions emit line radiation which leaves the optically thin plasma, thus contributing to the overall power loss. The electron temperature and density profiles are determined by measuring Doppler shifts, laser light scattering, and line emission intensities, while the distribution of ionic states may be studied by constructing a set of rate equations which require as input various atomic rates such as collisional excitation, ionization, radiative decay, and capture. In particular, capture of continuum electrons by ions may proceed either by a direct radiative recombination or, more frequently, by DR and its higher-order processes.

Precise calculations of the DR rate coefficients are lengthy and tedious due to the multistep nature of the process of free-electron capture into one of a doubly infinite set of intermediate excited states. These states may then either decay by Auger electron emission or radiatively decay to final states, which could themselves be unstable with respect to further Auger emission. Consequently, only a limited number of ions have been treated theoretically and various semiempirical formulas are employed for practical applications. Burgess proposed a phenomenological formula[2] for ions of $Z_C\lesssim 20$ where, at low temperatures, the $\Delta n=0$ process is dominant. Merts *et al.*[3] later modified the formula to incorporate the $\Delta n\neq 0$ transitions and considered the ions around $Z_C=26$, and an improved formula was recently proposed by Hahn.[4,5] To examine the effectiveness of these formulas it is necessary to have as benchmark cases several precise calculations of DR rate coefficients. To this end we report the results of a detailed calculation of the DR rate coefficients for the target ions of the Li isoelectronic sequence at several thermal energies. This paper extends the earlier study[6] of Fe^{23+} to the ions O^{5+}, Ar^{15+}, and Mo^{39+}. The calculational procedure is similar to that employed in the previous treatment of the He, Be, Ne, and Na sequences[4,5,7,8] except for an improved theoretical procedure for large n and l states. Both the $\Delta n=0$ $(2s\rightarrow 2p)$ and $\Delta n\neq 0$ $(1s\rightarrow nl$ with $n\geq 2$ and $2s\rightarrow n'l'$ with $n'\geq 3)$ transitions are involved; they are discussed separately in Sec. III, after a brief summary of the formalism in Sec. II. Because of the temperature-dependent (exponential) factor in the DR rate, the $\Delta n=0$ transition contributes most at low temperatures, the $2s$ excitation with $\Delta n\neq 0$ is dominant at medium temperatures, and the $1s$ excitation contribution is generally small except at relatively higher energies.

II. FORMALISM

The dielectronic-recombination process proceeds as

$$e+A(Z_C,Z_I)\rightarrow A^{**}(Z_C,Z_I-1)\rightarrow A^{*}(Z_C,Z_I-1)+\hbar\omega\ ,$$

where Z_C and Z_I are, respectively, the nuclear core charge and degree of ionization of the initial ion with the number of electrons $N=Z_C-Z_I$. $(N=3$ in this case.) The initial capture is a resonance process with conservation of energy and momentum, leading to a doubly excited autoionizing state A^{**}. The recombined ion A^* in the final state f may be unstable against further emission of photons (or Auger electrons). The DR rate coefficient in cm^3/sec for this process is defined by[9]

$$\alpha^{\mathrm{DR}}(d)\equiv\sum_{i,l_c}\alpha^{\mathrm{DR}}(i,l_c\rightarrow d)$$
$$=\left[\frac{4\pi Ry}{k_BT_e}\right]^{3/2}a_0^3e^{-e_c/k_BT_e}V_a(i,l_c\rightarrow d)\omega(d)\ , \quad (2.1)$$

where l_c and e_c are the angular momentum and energy of the continuum electron. The initial state of the target is labeled i, the doubly excited intermediate autoionizing state is denoted d, and a_0 is the atomic unit of length. The radiationless capture probability V_a ($\sec^{-1}$) is related to the inverse autoionization probability A_a ($\sec^{-1}$) by the principle of detailed balance

$$g_e g_i V_a(i, l_c \rightarrow d) = g_d A_a(d \rightarrow i, l_c) , \tag{2.2}$$

where g_d and g_i are the statistical weights of the states d and i, and $g_e = 2$ is the intrinsic (spin) weight of the continuum electron. The Auger probability is given by (in a.u.)

$$A_a(d \rightarrow i, l_c) = 2\pi \, | \langle i, l_c \, | \, V \, | \, d \rangle |^2 , \tag{2.3}$$

where V is the electron-electron interaction. The normalization of the continuum state is such that its radial part behaves asymptotically as

$$\phi_{e_c} = \left[\frac{2}{\pi k_c} \right]^{1/2} \frac{1}{r} \sin \left[k_c r - \frac{l_c \pi}{2} - \frac{Z_I}{k_c} \ln(2k_c r) + \sigma_{l_c} + \delta_{l_c} \right] , \tag{2.4}$$

where σ_{l_c} is the Coulomb phase shift given by

$$\sigma_{l_c} = \arg\Gamma(l_c + 1 + i/k_c)$$

and δ_{l_c} is the phase shift due to the Hartree-Fock potential of the core ion. The fluorescence yield $\omega(d)$ in Eq. (2.1) is defined (neglecting the cascade effect to be discussed later) as

$$\omega(d) = \frac{\Gamma_r(d)}{\Gamma_r(d) + \Gamma_a(d)} , \tag{2.5}$$

where the radiative decay width is

$$\Gamma_r(d) = \sum_f A_r(d \rightarrow f) \tag{2.6}$$

in which f denotes all the allowed states that are Auger stable. [Otherwise $\omega(d)$ in $\alpha^{\rm DR}$ has to be modified for the cascade effect.] The single-electron (spontaneous) radiative transition probability is, in a.u.)

$$A_r^{(0)}(d \rightarrow f) = \tfrac{4}{3} (\omega_{fd})^3 \, | \langle f \, | \, D \, | \, d \rangle |^2 . \tag{2.7}$$

In Eq. (2.7) D is the dipole coupling operator and we use the length form ($\sim \hat{e} \cdot \vec{r}$) throughout. The Auger width is

$$\Gamma_a(d) = \sum_i \sum_{l_c} A_a(d \rightarrow i, l_c) . \tag{2.8}$$

All possible states i that are connected to d through V which are allowed by energy conservation and angular momentum and parity selection rules are summed over.

For both the A_a and A_r the bound-state orbitals are computed numerically with the nonrelativistic, single-configuration, Hartree-Fock code of Froese-Fisher.[10] In particular, the A_a are evaluated in the distorted-wave Born approximation (DWBA) and the continuum wave function is calculated with the Hartree-Fock direct and explicit nonlocal exchange potentials.

We proceed by first calculating a complete set of transitions in an angular-momentum-averaged[4] (AMA) scheme which readily allows a great number of intermediate d states to be treated. This procedure is extremely simple but is generally known to overestimate the DR rate, sometimes by as much as a factor of 2.[9] A dominant set of transitions which usually includes about 70% or more of the total contribution is then reexamined for the effects of cascade, LS coupling, and configuration mixing. The total DR rate is then obtained by an appropriate scaling. The necessary formulas are given in the appendixes.

III. RESULTS OF THE CALCULATION

A. $2s$, $\Delta n \neq 0$ excitation

At low and medium temperatures the dominant mode of the DR process is $2s$-electron excitation in which the $2s$ and projectile electrons proceed to intermediate states of the form

$$1s^2 2s + e_c l_c \overset{V_a}{\rightarrow} 1s^2 (n_a \, l_a)(n_b l_b) \overset{A_r}{\rightarrow} f + \hbar\omega \tag{3.1}$$

with the approximate resonance condition

$$e_i + e_c \approx e_{n_a l_a} + e_{n_b l_b}$$

and where $n_a \geq 3$ and $n_b \geq n_a$ for the $\Delta n \neq 0$ process. For $n_a = 2$ and $l_a = 1$ we have the $\Delta n_a = 0$ process which will be discussed in Sec. III B. The calculational procedure employed here is similar to that of the previous investigations of the Ne and Be isoelectronic sequences, except for the treatment of the O^{5+} system. That is, for the Ar, Fe, and Mo targets, a dominant set of these transitions (about 70% of the $2s$ $\Delta n_a \neq 0$ rate) is selected from the previous study of the $Fe^{23+} + e$ system and the rate coefficient for this set is calculated in an explicit LS-coupling scheme in which the spin and orbital angular momenta of the active pair of electrons, L_{ab} and S_{ab}, are specified. For a given intermediate state d, a rate coefficient is calculated for each allowed value of L_{ab} and S_{ab}. The state d is specified in the present case by ($n_a l_a$, $n_b l_b$, $L_{ab} = L = l_c$; $S_{ab} = S = 0$ or 1). The rate coefficient for the d state is then obtained by summing the rates for each allowed value of L_{ab} and S_{ab}. In this manner we obtain a subtotal $\alpha^{\rm DR}_{\rm dom}(\text{ion}, LS)$ for each member of the sequence. The total rate for each ion is then obtained by simply scaling from the $Fe^{23+} + e$ result:

$$\alpha^{\rm DR}_{\rm tot}(\text{ion}, LS) = \alpha^{\rm DR}_{\rm dom}(\text{ion}, LS) R(Fe^{23+}) \tag{3.2}$$

with

$$R(Fe^{23+}) = \frac{\alpha^{\rm DR}_{\rm tot}(Fe^{23+}, \text{AMA})}{\alpha^{\rm DR}_{\rm dom}(Fe^{23+}, \text{AMA})} , \tag{3.3}$$

where we assumed that R is unchanged for ions of a given isoelectronic sequence, providing that the ions are not too widely separated in Z_C from Fe,

$$R(Fe^{23+}) \approx R(Mo^{39+}) \approx R(Ar^{15+}) . \quad (3.4)$$

This also requires the thermal energy factor $k_B T_e$ to be scaled as an effective charge Z with $Z_I < Z < Z_C$ so that the Maxwellian distribution factor $\exp(-e_c/k_B T_e)$ is approximately the same for the ions of the sequence. Here Z is taken to be roughly $Z=(Z_I+Z_C)/2$ and $k_B T_e = 1$, 2, 4, and 8 keV for Fe^{23+}. The $O^{5+}+e$ system is an exception; it is sufficiently different from the other ions of the sequence that the total $2s$ $\Delta n \neq 0$ transition rate is explicitly calculated without resort to scaling.

The rate coefficients are calculated for the states $n_a = 3,4$ with $n_b = 3$ to 6 or 7 and the contribution of the high n_b tail ($n_b > 7$) is obtained by fitting $\Gamma_r(d)$ and $\Gamma_a(d)$ as functions of n_b.[11] For fixed n_a both A_a and A_r are proportional to $1/n_b^3$ for large n_b as specified by bound-state wave-function normalization. Thus we have

$$\Gamma_r(d) \sim a + b/n_b^3 , \quad (3.5)$$

$$\Gamma_a(d) \sim c + d/n_b^3 , \quad (3.6)$$

where the constants a, b, c, and d are determined for each particular intermediate state. The constants a and c represent those radiative and Auger transitions that do not depend upon n_b. Then with Eq. (2.5) we have

$$\omega(n_b) = n_b^3 \left[\frac{1+(b/a)/n_b^3}{(1+c/a)n_b^3+(b+d)/a} \right] . \quad (3.7)$$

Apparently, the dependence of α^{DR} on n_b can be much weaker than $1/n_b^3$ if $\omega(d)$ is strongly n_b dependent. This is the case for light ions and for ions in which one electron is captured into a high Rydberg state. We find that $\alpha^{DR}(n_b)$ is roughly constant until $n_b \approx \bar{n}_b = [(b+d)/a]^{1/3}$ beyond which point $\alpha^{DR}(n_b) \sim 1/n_b^3$. The results of the calculation are summarized in Table I. The summation over n_b in the evaluation of α^{DR} is carried out by an approximate formula

$$\alpha^{DR}(d) \equiv \sum_{n_b=3}^{\infty} \alpha^{DR}(n_a l_a, n_b l_b) = \sum_{n_b=3}^{n_0-1} \alpha^{DR}(n_a l_a, n_b l_b) + \sum_{n_b=n_0}^{\infty} \beta_0(n_a l_a) \left[\frac{1+(b/a)/n_b^3}{(1+c/a)n_b^3+(b+d)/a} \right] , \quad (3.8)$$

where n_0 is roughly equal to $\lesssim 2l$. ($n_0 \approx 6$–10 for $\Delta n \neq 0$ transitions.) Typically, $n_b \lesssim 20$ are involved. Contributions from $n_a \geq 4$ are small.

B. $2s$, $\Delta n = 0$ excitation

The initial state $1s^2 2s$ can be excited to the configuration $1s^2 2p$ by low-energy electrons which are captured into high Rydberg states without radiation emission. We have

$$1s^2 2s + e_c l_c \xrightarrow{V_a} 1s^2 2p n_b l_b \begin{cases} \xrightarrow{A_r} 1s^2 2p(n_f l_f) + \hbar\omega \\ \rightarrow 1s^2 2s(n_b l_b) + \hbar\omega' \end{cases}$$

with the resonance condition

$$e_c + e_{2s} \cong e_{2p} + e_{n_b l_b} ,$$

or more accurately $e_c + E_i = E_f$ where the E's represent the total energy. Therefore, the threshold value for n_b is determined by the energy separation between the $1s^2 2s$ and $1s^2 2p$ states. It is obtained from the nonrelativistic Hartree-Fock code and further adjusted using the table of Cheng *et al.*[12] The lowest allowed value of n_b (for which $e_c = 0$) is $n_b = 6$ for O^{5+}, $n_b = 10$ for Ar^{15+}, and $n_b = 12$ for both Fe^{23+} and Mo^{39+} corresponding to $(2s \rightarrow 2p) = 0.889$, 2.51, 4.35, and 12.5 Ry, respectively.

TABLE I. DR rate coefficients α^{DR} are listed for a representative group of $\Delta n \neq 0$ transitions. All allowed Auger decays are included in the calculation. $k_B T_e$ is at 5.17 Ry for O^{5+}, 33.3 Ry for Ar^{15+}, 73.5 Ry for Fe^{23+}, 200.8 Ry for Mo^{39+}.

d	l_c	O^{5+}	Ar^{15+}	Fe^{23+}	Mo^{39+}
$3snp$	1	0.598	2.17	3.71	2.89
$3snd$	2	2.88	7.85	10.2	7.04
$3snf$	3	0.786	5.35	3.73	1.62
$3dnd$	4	0.442	2.69	3.20	3.62
$3dnf$	5	0.867	10.7	8.73	4.97
$3dng$	6	0.462	4.36	4.41	1.45
Sum		6.04	33.1	34.0	21.6
Extrapolated total		14.9	76.4	74.6	48.6
Cascade reduction		14.9	68.9	66.2	46.4

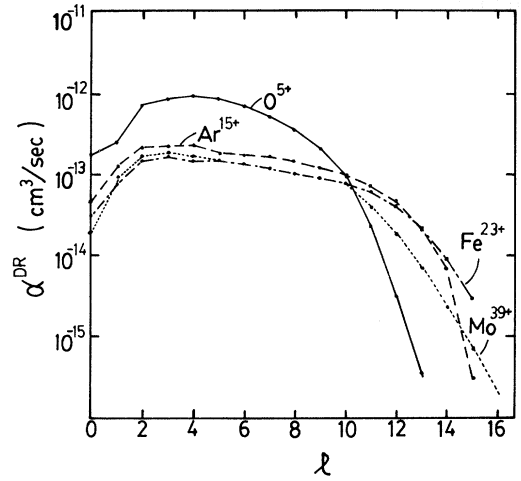

FIG. 1. DR rate coefficients $\sum_{l_c}\sum_{n_b=n_m}^{\infty}\alpha^{DR}(1s^22s+e_cl_c\rightarrow 1s^22pn_bl_b)$ vs $l_b\equiv l$, $L_{ab}S_{ab}$-coupling results in units of cm^3/sec. k_BT_e for O^{5+} is at 5.17 Ry, 33.3 Ry for Ar^{15+}, 73.5 Ry for Fe^{23+}, 200.8 Ry for Mo^{39+}.

(These values are weighted averages of $J=\frac{1}{2}$ and $J=\frac{3}{2}$ levels.) The method of calculation is described in Sec. III A. The large-n_b contribution is dominant for the present $\Delta n_a=0$ transitions, with contributions coming from $n_b\lesssim 300$ for O^{5+}, $n_b\lesssim 200$ for Ar^{15+}, $n_b\lesssim 150$ for Fe^{23+}, and $n_b\lesssim 80$ for Mo^{39+}. Equation (3.8) is used to sum these contributions. Eventually these high Rydberg state contributions will be truncated by the density and field effects but we do not consider that problem here. The contributions from high l_b are found to be important and were explicitly evaluated for $l_b\leq 15$. For $l_b>15$ the DR rates are approximated with a simple Gaussian fit.[13] The results of the calculation are summarized in Fig. 1 where the rate coefficient

$$\sum_{l_c}\sum_{n_b}\alpha^{DR}(1s^22s+e_cl_c\rightarrow 1s^22pn_bl_b)$$

is plotted versus l_b. , the high l_b contribution is more important for heavier ions than for lighter ions in which case $l_b\lesssim 10$ may be sufficient. The high-n_b ($n_b>15$) contribution is estimated in the direct, dipole approximation without exchange for A_a, and in the Coulomb approximation for A_r. The accuracy of this approximation has been checked with explicit calculations.

It is of interest to note that the $\Delta n_a=0$ transitions have been recently investigated experimentally.[14] The B^{2+} and C^{3+} targets were used in a merged electron-ion beam apparatus to measure the DR cross section. The comparison with our distorted-wave calculations[15,16] is in reasonable agreement after cutting off the high-n_b tail contribution at $n_b=22$ and 26 for B^{2+} and C^{3+}, respectively. After folding the theoretical cross sections over a beam profile of 2.0 eV the Oak Ridge group[16] obtained an effective cross section ratio of 2.3 ± 0.3 while our estimate gave

$$\sum_{l_b=0}^{n_b-1}\sum_{n_b=4}^{26}\bar{\sigma}^{DR}(C^{3+})\Big/\sum_{l_b=0}^{n_b-1}\sum_{n_b=4}^{22}\bar{\sigma}^{DR}(B^{2+})=1.5\ .$$

It should be noted that only the last bin of the cross-section space is convolved in the theoretical prediction of the effective cross section and that folding in the other peaks could raise the predicted cross section by about 10%. The Burgess-Merts theory predicts essentially the same ratio of 1.5. The scaling property of the DR cross section in the effective charge Z has been examined recently for $\Delta n=0$ transitions and the results will be published elsewhere.

C. 1s excitation

The rate coefficient for 1s transitions is generally small at low temperatures due to the large 1s excitation energy which, in turn, results in large e_c in the exponential factor $\exp(-e_c/k_BT_e)$. However, we find that as much as 40% of the total DR rate coefficient comes from the 1s excitation at high temperatures. The dominant 1s transitions are

$$1s^22s+e_c(s,d)\rightarrow 1s\,2s\,2pn_bp\ ,$$

$$1s^22s+e_c(p,f)\rightarrow 1s\,2s\,2pn_bd\ ,$$

and are estimated to contribute 90% of the total 1s transition rate for Fe and Mo ions according to the Fe^{23+} result.[6] The previous study of the He sequence[11] indicates that for lighter ions the $1s\rightarrow 2p$ transition is less important. There is no large-n_b tail contribution for this process because of the presence of the additional Auger channel

$$1s\,2s\,2pn_bl_b\xrightarrow{A_a}1s^2n_bl_b+e_c'l_c'\ .$$

The A_a for this process dominates the Auger width and remains constant as n_b increases along a Rydberg series, resulting in a small but constant value for the fluorescence yield, $\omega(d)$. Consequently, $\alpha^{DR}(n_b)$ scales as $1/n_b^3$. The total 1s transition rate is given for the different ions in Figs. 2–5. The result for the 1s transition is compared with the earlier calculation[5] and found to be consistent

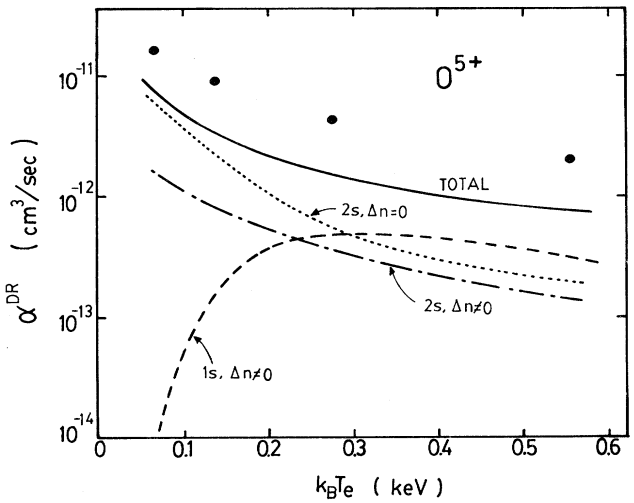

FIG. 2. *LS*-coupled, cascade-corrected rate coefficients are given as a function of electron temperature for O^{5+}. Circles are predicted total rates obtained from the Burgess-Merts formula (Hulse version).

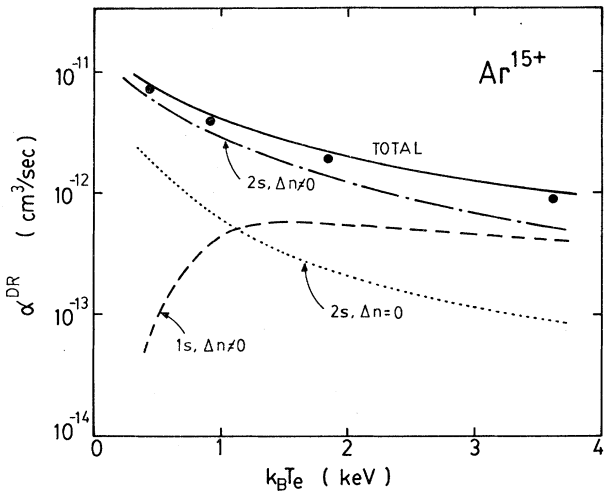

FIG. 3. *LS*-coupled, cascade-corrected rate coefficients are given as a function of electron temperature for Ar^{15+}.

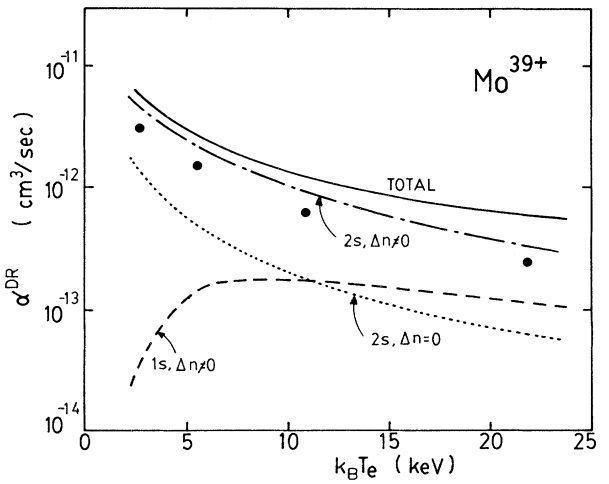

FIG. 5. *LS*-coupled, cascade-corrected rate coefficients are given as a function of electron temperature for Mo^{39+}

with the same $1s$ excitation in the Be and the He sequences[5,7] when the effects of the additional spectator electrons are taken into account.

Incidentally, we note that the $1s$ excitation has been used by Tanis *et al.*[17] in their study of the resonant transfer excitation (RTE) process in ion-atom collisions. Thus, for example, in the S^{11+} + Ar collision the M-shell electrons of the Ar atoms are assumed to provide the electron "beam," which excites the $1s$ electron in S^{11+}. Their RTE cross section was found to be about a factor of 2 larger than our explicit calculation of the DR cross section[18] after folding the cross section over the Compton profile of the Ar atoms. Due to uncertainty in the role played by these electrons, as well as by the Ar core nucleus, it is not clear whether the resonance structure seen in the experiment in fact represents DR. A certain fraction of the K x ray observed in coincidence with the charge-exchanging S ion should come from the DR-like process, but more theoretical and experimental study is needed to clarify the situation.

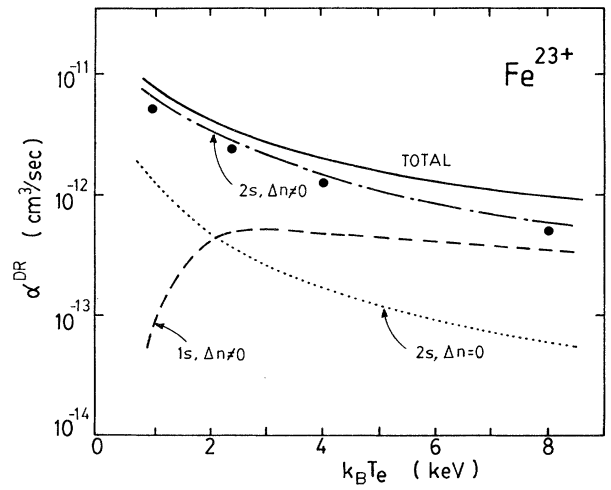

FIG. 4. *LS*-coupled, cascade-corrected rate coefficients are given as a function of electron temperature for Fe^{23+}.

IV. CASCADE CORRECTION

The cascade effect arises from the fact that the intermediate states d formed by the initial collisional excitation may radiatively decay to states d' which can further decay by Auger emission. The fluorescence yield Eq. (2.5) is modified[9] as

$$\omega(d)=\frac{1}{\Gamma_r(d)+\Gamma_a(d)} \times\left[\sum_f A_r(d\to f) + \sum_{d',f}\frac{A_r(d\to d')A_r(d'\to f)}{\Gamma_r(d')+\Gamma_a(d')}+\cdots\right]. \quad (4.1)$$

The states labeled f are stable with respect to electron emission and the states labeled d' are Auger unstable. (The states labeled d can, of course, also decay either by photon or electron emission.) Consider, for example, the $2s$ $\Delta n\neq 0$ excitation-capture to the intermediate state $d=1s^2 3s\,4d$ in the $Ar^{15+}+e$ system. This state (d) will subsequently decay either by radiative emission (with rates A_r) or by Auger emission (with rates A_a). In the single-configuration, dipole approximation we have

$$\begin{matrix} i_1 & 1s^2 2s + e_c l_c \\ i_2 & 1s^2 2p + e_c' l_c' \end{matrix} \overset{V_a}{\underset{A_a}{\rightleftarrows}} 1s^2 3s\,4d \xrightarrow{A_r} \begin{cases} 1s^2 2p\,4d & f_1 \\ 1s^2 2p\,3s & f_2 \\ 1s^2 3s\,3p & f_3 \\ 1s^2 3s\,4p & f_4 . \end{cases}$$

The states f_3 and f_4 can, in turn, further radiatively decay or Auger decay to the states i_1+e_c'' or i_2+e_c'''. Thus the contributions of $A_r(d\to f_3)$ and $A_r(d\to f_4)$ to $\omega(d)$ are reduced by the factors $\omega(f_3)$ and $\omega(f_4)$, respectively. On

the other hand, the states f_1 and f_2 have no available Auger channels and consequently $A_r(d \rightarrow f_1)$ and $A_r(d \rightarrow f_2)$ contribute to $\omega(d)$ in full strength. This reduces the overall fluorescence yield and thus the rate α^{DR}. We have estimated the cascade effect for several dominant $2s$ $\Delta n \neq 0$ transitions and the result is summarized as a reduction factor in Table I for the ions Ar^{15+}, Fe^{23+}, and Mo^{39+}. The cascade effect is directly incorporated in the calculation of the O^{5+} system by simply deleting those radiative transition probabilites to final states which are Auger unstable in the numerator of $\omega(d)$. This is a good approximation because $\Gamma_a(d) \gg \Gamma_r(d)$ and thus $\omega \ll 1$ for O^{5+}. The cascade effect is negligible for the dominant $1s$ transitions which are predominantly stabilized by the $2p \rightarrow 1s$ radiative transitions. In general, the effect is difficult to estimate, particularly when the electrons are in high Rydberg states since the A_a and A_r are required for many d', f', and i'. Each individual case is carefully estimated in the present calculation.

V. EFFECTS OF CONFIGURATION INTERACTION

Atomic states belonging to different configurations that have the same values of L and S and the same parity become mixed because the one-electron orbital angular momentum operators do not commute with the electron-electron interaction. Improved states can then be constructed by the configuration-interaction expansion

$$\Psi^{\mathrm{CI}}(LS) = \sum_p a_{qp} \phi_p(LS) , \tag{5.1}$$

where L and S are the total orbital and spin angular momenta and p is summed over the number of configurations in the expansion (two in this investigation). The basis set of single-configuration wave functions, $\{\phi_p(LS)\}$, is generated by the nonrelativistic Hartree-Fock Hamiltonian and the coefficients a_{qp} are obtained by diagonalizing the matrix $\underline{V}$, with matrix elements $V_{qp} = \langle \phi_q \mid e^2/r_{12} \mid \phi_p \rangle$, as

$$\underline{V}^D = \underline{A}^T \underline{V} \underline{A} . \tag{5.2}$$

The effect of configuration interaction on the DR rate coefficient is examined by using the improved states d^{CI} of the form $\Psi^{\mathrm{CI}}(LS)$ in the evaluation of V_a and $\omega(d)$. A rate coefficient is then calculated for each d^{CI} and the sum $\sum_d \alpha^{\mathrm{DR}}_{\mathrm{CI}}(d)$ is obtained. The result is compared to the sum of the DR rates for the same set of transitions calculated in the LS-coupled, single-configuration approximation. Some sample cases are given in Table II. The most strongly coupled d states of the dominant transitions are included which constitute about 12% of the total $2s$ $\Delta n \neq 0$ transition rate. Most of the dominant transitions are found to be only weakly mixed and thus are not affected by the configuration interaction. These rates are to be compared with the single-configuration LS-coupled, term-specific rate coefficients presented in Table III. We find that although configuration mixing of the d state can change individual rate coefficients by as much as 30%, the net change in the rate coefficient for this subset of states when summed over all LS terms is only about 5% because of the apparently random changes (some increasing, some decreasing) in the configuration-mixed rates. This conclusion is consistent with the earlier work of Roszman and Weiss[19] and LaGatutta.[20]

TABLE II. Fluorescence yields and DR rate coefficients (cm^3/sec) are given for a set of $\Delta n \neq 0$ transitions for the Fe^{23+} target ion at 1 keV in the single-configuration LS basis. Numbers in parentheses are powers of ten, e.g., $2.01(-13) = 2.01 \times 10^{-13}$.

Configuration	State	$\omega(d)$	α^{DR}
$3s\,3d$	^1D	0.0739	2.01(−13)
$3p^2$	^1D	0.0404	4.65(−15)
$3d^2$	^1D	0.0822	1.45(−14)
$3s\,4p$	^1P	0.0690	1.70(−14)
$3s\,4p$	^3P	0.1353	4.46(−14)
$3s\,4d$	^1D	0.1049	6.46(−14)
$3s\,4d$	^3D	0.4027	1.11(−13)
$3p\,4s$	^1P	0.0833	1.39(−14)
$3p\,4s$	^3P	0.1993	3.04(−14)
$3p\,4d$	^1P	0.1989	7.32(−15)
$3p\,4d$	^3P	0.3247	3.46(−16)
$3d\,4s$	^1D	0.1663	8.38(−14)
$3d\,4s$	^3D	0.7732	2.36(−14)
$3d\,4p$	^1P	0.1455	6.55(−15)
$3d\,4p$	^3P	0.4470	2.48(−15)

VI. SUMMARY

The LS-coupled, cascade-corrected results for each transition and the total DR rates for each ion are summarized graphically in Figs. 2–5 as a function of $k_B T_e$. The core charge dependence of the DR rates for the lithium se-

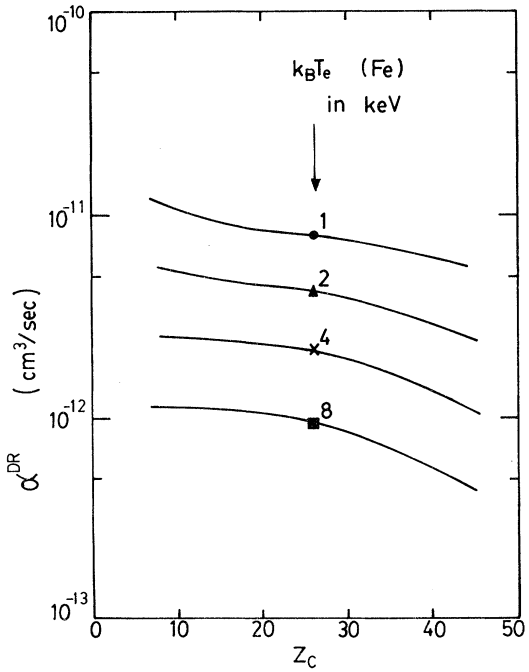

FIG. 6. Core charge dependence of the DR rates for the lithiumlike sequence is presented with the $k_B T_e$ values scales as Z^2 and centered on 1, 2, 4, and 8 keV for Fe^{23+}.

TABLE III. Mixing coefficients, fluorescence yields, and DR rate coefficients (cm^3/sec) are given for the same set of transitions as are in Table II for comparison. (Fe^{23+} ion at 1 keV.) Numbers in parentheses are powers of ten, e.g., $1.56(-14)=1.56\times10^{-14}$.

q	Configuration	State	a_{q2}	a_{q1}	$\omega^{CI}(d)$	$\alpha_{CI}^{DR}(d)$
1	$3s\,4p$	$1P$	0.535 39	0.844 60	0.0422	1.56(−14)
2	$3p\,4s$	$1P$	0.844 60	−0.535 39	0.3632	1.33(−14)
1	$3s\,4p$	$3P$	0.543 06	0.839 70	0.5654	3.09(−16)
2	$3p\,4s$	$3P$	0.839 70	−0.543 06	0.0882	4.15(−14)
1	$3s\,4p$	$1P$	−0.288 75	0.957 40	0.1270	7.65(−17)
2	$3p\,4d$	$1P$	0.957 40	0.288 75	0.0443	1.31(−14)
1	$3s\,4p$	$3P$	−0.295 84	0.955 24	0.3880	8.05(−15)
2	$3p\,4d$	$3P$	0.955 24	0.295 84	0.1170	3.83(−14)
1	$3s\,4p$	$1P$	0.140 45	0.990 09	0.2275	2.32(−14)
2	$3d\,4p$	$1P$	0.990 09	−0.140 45	0.0790	1.66(−14)
1	$3s\,4p$	$3P$	0.138 32	0.990 39	0.4260	1.11(−14)
2	$3d\,4p$	$3P$	0.990 39	−0.138 32	0.1099	3.44(−14)
1	$3s\,3d$	$1D$	0.664 02	0.747 71	0.0486	9.32(−14)
2	$3p^2$	$1D$	0.747 71	−0.664 01	0.0702	7.80(−14)
1	$3s\,3d$	$1D$	−0.307 82	0.951 44	0.1060	1.18(−15)
2	$3d^2$	$1D$	0.951 44	0.307 82	0.0629	1.89(−13)
1	$3d^2$	$1D$	−0.542 03	0.840 36	0.0687	2.01(−14)
2	$3p^2$	$1D$	0.840 36	0.540 23	0.1340	9.59(−16)
1	$3s\,4d$	$1D$	0.608 15	0.793 82	0.1056	1.17(−13)
2	$3d\,4s$	$1D$	0.793 82	−0.608 15	0.6132	3.65(−14)
1	$3s\,4d$	$3D$	0.601 13	0.799 15	0.8778	3.99(−14)
2	$3d\,4s$	$3D$	0.799 15	−0.601 13	0.4723	1.67(−13)
1	$3s\,4d$	$1D$	0.502 93	0.864 33	0.0972	3.11(−14)
2	$3p\,4p$	$1D$	0.864 33	−0.502 93	0.1272	4.39(−14)
1	$3s\,4d$	$3D$	0.461 38	0.887 20	0.6633	4.81(−14)
2	$3p\,4p$	$3D$	0.887 20	−0.461 38	0.4464	1.07(−13)
1	$3p\,4p$	$1D$	0.564 94	0.825 14	0.1363	1.01(−13)
2	$3d\,4s$	$1D$	0.825 14	−0.564 94	0.2066	3.75(−14)
1	$3p\,4p$	$3D$	0.657 24	0.753 68	0.7146	2.33(−14)
2	$3d\,4s$	$3D$	0.753 68	−0.657 24	0.7238	2.13(−14)

quence is presented in Fig. 6 with the k_BT_e values scaled as Z^2 and centered on 1, 2, 4, and 8 keV for the Fe^{23+} ion. This is the first comprehensive treatment of the dielectronic-recombination rate for the Li sequence and, together with the previous results for the H, He, Be, Ne, and Na isoelectronic sequences, should be useful in improving existing phenomenological formulas. This calculation does not include the effect of intermediate coupling, relativistic effects, or the density and field effects. It should be noted that collisional and Stark mixing of levels due to charged particles and applied fields in the plasma may seriously alter the capture rate. These important corrections are being investigated and the details of these more-precise calculations are forthcoming. In the course of this study many intermediate results have been obtained on A_r, A_a, $\omega(d)$, etc. which would be useful for spectral analysis and autoionization studies. These data are being compiled for publication elsewhere.

ACKNOWLEDGMENTS

We would like to thank Dr. K. J. LaGattuta for many helpful discussions on various aspects of the present study and I. Nasser for computational assistance. Dr. R. Hulse of the Princeton Plasma Physics Laboratory kindly supplied us with the semiempirical rates for comparison. The work reported here has been supported in part by the U.S. Department of Energy under Contract No. DE-AC02-76ET3035. D. J. M. also acknowledges summer fellowship support for two years and generous additional grants by the University of Connecticut Research Foundation. The calculation was carried out at the University of Connecticut Computer Center, which has been supported in part by a National Science Foundation grant, and we appreciate their assistance in providing computer time for this research. This work was submitted to the University of Connecticut in partial fulfillment for the requirement for the Ph.D. degree.

APPENDIX A

The Auger transition probability is defined in an explicit LS-coupling scheme. We distinguish two cases depending on whether spectator electrons in an unfilled shell occur in the transition. The first case is defined for $2s$ (or $2p$) transitions as

$$A_a(n_a l_a, n_b l_b \rightarrow n_s l_s, e_\gamma l_\gamma) = \frac{1}{N_{ab}} \hat{l}_a \hat{l}_b \hat{l}_s \hat{l}_\gamma I^2(L_{ab} S_{ab}) ,$$

where $N_{ab}=1$ if $(n_a l_a) \neq (n_b l_b)$ and $N_{ab}=2$ if $(n_a l_a)=(n_b l_b)$, $\hat{l}=2l+1$, and

$$I(L_{ab}S_{ab}) = \sum_k R_k(l_s l_\gamma l_a l_b) \begin{bmatrix} l_s & k & l_a \\ 0 & 0 & 0 \end{bmatrix} \begin{bmatrix} l_\gamma & k & l_b \\ 0 & 0 & 0 \end{bmatrix} \begin{Bmatrix} l_s & l_a & k \\ l_b & l_\gamma & L_{ab} \end{Bmatrix}$$
$$+(-1)^{L_{ab}-S_{ab}} \sum_{k'} R_{k'}(l_s l_\gamma l_b l_a) \begin{bmatrix} l_s & k' & l_b \\ 0 & 0 & 0 \end{bmatrix} \begin{bmatrix} l_\gamma & k' & l_a \\ 0 & 0 & 0 \end{bmatrix} \begin{Bmatrix} l_s & l_b & k' \\ l_a & l_\gamma & L_{ab} \end{Bmatrix} ,$$

where the R_k are the usual radial integrals

$$R_k(l_s l_\gamma l_a l_b) = \int\int dr_1\, r_1^2\, dr_2\, r_2^2 \phi_\gamma(r_1)\phi_s(r_2) \left[\frac{r_<^k}{r_>^{k+1}} \right] \phi_a(r_1)\phi_b(r_2) .$$

The second case treats intermediate states of the form ($1s$ transitions)

$$\phi_d = \{(n_s l_s)^m (n_d l_d)[L_{sd}S_{sd}], (n_a l_a)(n_b l_b)[L_{ab}S_{ab}], LS\}$$

which is valid for $m+1=4l_s+2$. We have the following for $A_a = A_a(L_{sd}S_{sd}L_{ab}S_{ab}LS)$:

(i) $\phi_d \rightarrow (n_s l_s)^{m+1}(n_d l_d) + e_\gamma l_\gamma$, $a \neq d$ and $b \neq d$,

$$A_a = \frac{1}{N_{ab}} \hat{l}_a \hat{l}_b \hat{l}_s \hat{l}_\gamma \hat{L}_{sd} \hat{S}_{sd} \hat{L}_{ab} \hat{S}_{ab} \begin{Bmatrix} L_{ds} & L & L_{ab} \\ l_\gamma & l_s & l_d \end{Bmatrix}^2 \begin{Bmatrix} S_{sd} & S & S_{ab} \\ \frac{1}{2} & \frac{1}{2} & \frac{1}{2} \end{Bmatrix}^2 I^2(L_{ab}, S_{ab}) ;$$

(ii) $\phi_d \rightarrow (n_s l_s)^{m+1}(n_a l_a) + e_\gamma l_\gamma$, $a \neq d$, $b \neq d$, and $l_d = 0$,

$$A_a = N_{ab} \hat{l}_s \hat{l}_b^2 \hat{l}_\gamma \hat{S}_{sd} \hat{L}_{ab} \hat{S}_{ab} \begin{Bmatrix} l_s & L_{ab} & L \\ l_a & l_\gamma & l_b \end{Bmatrix}^2 \begin{Bmatrix} S_{sd} & S_{ab} & S \\ \frac{1}{2} & \frac{1}{2} & \frac{1}{2} \end{Bmatrix}^2 \left| \sum_{S_{db}} \hat{S}_{db} \begin{Bmatrix} \frac{1}{2} & \frac{1}{2} & S_{db} \\ \frac{1}{2} & \frac{1}{2} & S_{sd} \end{Bmatrix} I(l_b, S_{db}) \right|^2 ;$$

(iii) $\phi_d \rightarrow (n_s l_s)^m (n_d l_d)^2 + e_\gamma l_\gamma$, $l_d = 0$,

$$A_a = \hat{l}_a \hat{l}_b \hat{l}_\gamma \hat{S}_{sd} \hat{S}_{ab} \begin{Bmatrix} S_{sd} & S_{ab} & S \\ \frac{1}{2} & \frac{1}{2} & \frac{1}{2} \end{Bmatrix}^2 I^2(L_{ab}, S_{ab}) \delta(L_{ab}, l_\gamma) ;$$

(iv) $\phi_d \rightarrow (n_s l_s)^m (n_d l_d)(n_e l_e) + e_\gamma l_\gamma$, $e \neq d$,

$$A_a = \hat{l}_a \hat{l}_b \hat{l}_e \hat{l}_\gamma I^2(L_{ab}, S_{ab}) .$$

APPENDIX B

In the following four cases, the radiative transition probabilities are defined in terms of the one-electron radiative probability $A_r^{(0)}$.

In case 1

$$(n_s l_s)^m (n_a l_a)(n_b l_b) \xrightarrow{A_r} (n_s l_s)^m (n_a l_a)(n_e l_e)$$

with $a \neq b$, $a \neq e$, $e \neq b$

$$A_r(L_{ab}S_{ab}LS) = A_r^{(0)} .$$

In case 2

$$(n_s l_s)^m (n_a l_a)(n_b l_b) \rightarrow (n_s l_s)^m (n_a l_a)^2, \quad a \neq b;$$

$$A_r(L_{ab}S_{ab}LS) = 2\hat{l}_b \sum_{\substack{L_{aa}, S_{aa} \\ (L_{aa}+S_{aa}=\text{even})}} \delta_{S_{aa}, S_{ab}} \hat{L}_{aa} \times \begin{Bmatrix} l_b & L_{ab} & l_a \\ L_{aa} & l_a & 1 \end{Bmatrix}^2 A_r^{(0)} .$$

In case 3

$$(n_s l_s)^m (n_a l_a)^2 \rightarrow (n_s l_s)^m (n_a l_a)(n_b l_b), \quad a \neq b$$

$$A_r(L_{aa} S_{aa} LS) = 2A_r^{(0)} .$$

In case 4

$$(n_s l_s)^m (n_d l_d)(n_a l_a)(n_b l_b) \rightarrow (n_s l_s)^{m+1} (n_d l_d)(n_a l_a)$$

with $m+1 = 4l_s + 2, \quad l_d = 0$

$$A_r(L_{sd} S_{sd} L_{ab} S_{ab} LS) = \frac{N_{ab}}{\hat{l}_s} \hat{l}_a \hat{L}_{sd} \hat{S}_{sd} \hat{L}_{ab} \hat{S}_{ab} \times \begin{Bmatrix} S_{sd} & S & S_{ab} \\ \frac{1}{2} & \frac{1}{2} & \frac{1}{2} \end{Bmatrix}^2 \begin{Bmatrix} L_{ab} & l_b & l_a \\ 1 & L & l_s \end{Bmatrix}^2 A_r^{(0)} ,$$

where in the dipole-nonretardation approximation for the transition $d \rightarrow f$

$$A_r^{(0)} = \frac{4}{3} \left[\frac{\hbar \omega_{fd}}{\alpha mc^2} \right]^3 | \langle n_f l_f | \hat{\epsilon} \cdot \vec{r} | n_d l_d \rangle |^2$$

$$= \frac{4}{3} \left[\frac{\hbar \omega_{fd}}{\alpha mc^2} \right]^3 \frac{l_>}{2l_d + 1} R_D^2$$

with

$$R_D(n_f l_f n_d l_d) = \int r^2 dr \phi_{n_f l_f}(r) r \phi_{n_d l_d}(r) .$$

[1] E. Hinnov, Phys. Rev. A 14, 1533 (1976).
[2] A. Burgess, Astrophys. J 141, 1588 (1965).
[3] A. L. Merts, R. D. Cowan, and N. H. Magee, Jr., Los Alamos Scientific Laboratory Report No. LA-6220-MS (unpublished).
[4] J. N. Gau, Y. Hahn, and J. A. Retter, J. Quant. Spectrosc. Radiat. Transfer 23, 65 (1980); 24, 505 (1980).
[5] Y. Hahn, Phys. Rev. A 22, 2896 (1980).
[6] D. J. McLaughlin and Y. Hahn, J. Quant. Spectrosc. Radiat. Transfer 28, 343 (1982).
[7] I. Nasser and Y. Hahn, J. Quant. Spectrosc. Radiat. Transfer 29, 1 (1983).
[8] K. J. LaGatutta and Y. Hahn (unpublished).
[9] J. N. Gau and Y. Hahn, J. Quant. Spectrosc. Radiat. Transfer 23, 147 (1980).
[10] C. Froese-Fisher, *The Hartree-Fock Method for Atoms* (Wiley, New York, 1977).
[11] K. J. LaGatutta and Y. Hahn, Phys. Lett. 84A, 468 (1981).
[12] K. T. Cheng, Y. K. Kim, and J. P. Desclaux, At. Data Nucl. Data Tables 24, 111 (1979).
[13] J. N. Gau and Y. Hahn, Phys. Lett. 68A, 197 (1978).
[14] P. F. Dittner, S. Datz, P. D. Miller, C. D. Moak, P. H. Stelson, C. Bottcher, W. B. Dress, G. D. Alton, and N. Neskovic, Phys. Rev. Lett. 51, 31 (1983).
[15] D. J. McLaughlin and Y. Hahn, Phys. Rev. A 27, 1389 (1983).
[16] D. J. McLaughlin and Y. Hahn, Phys. Rev. A 28, 493 (1983).
[17] J. A. Tanis, E. M. Bernstein, W. G. Graham, M. Clark, S. M. Shafroth, B. M. Johnson, K. W. Jones, and M. Meron, Phys. Rev. Lett. 49, 1325 (1982).
[18] D. J. McLaughlin and Y. Hahn, Phys. Lett. 88A, 394 (1982).
[19] L. Roszman and A. Weiss, J. Quant. Spectrosc. Radiat. Transfer 30, 67 (1983).
[20] K. J. LaGatutta (private communication).